

Molecular Engineering of Coupled Polynuclear Systems: Orbital Mechanism of the Interaction between Metallic Centers

OLIVIER KAHN

Laboratoire de Spectrochimie des Eléments de Transitions, Equipe de Recherche Associée au CNRS No 672, Université de Paris-Sud, 91405 Orsay, France

Received January 23, 1982

The aim of this work was to propose a strategy allowing the synthesis of polynuclear complexes with expected magnetic properties. First, we recall the broad outlines of an orbital model for describing the exchange interaction in coupled systems. This model is grounded on the concepts of magnetic orbitals and of overlap density between magnetic orbitals. Then we focus on two problems, namely the design of ferromagnetically-coupled systems and the design of binuclear complexes exhibiting a very large antiferromagnetic interaction between metal ions far away from each other.

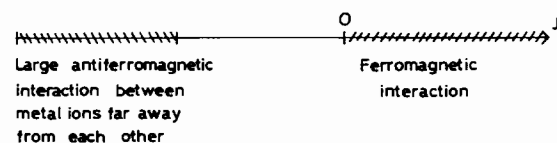
When the overlap between the magnetic orbitals is zero, the antiferromagnetic contribution is also zero and the coupling is purely ferromagnetic. Two strategies may be used to obtain this result, either the strict orthogonality or the accidental orthogonality. The strict orthogonality is realized in $\text{CuVO}(\text{fsa})_2\text{en}$, CH_3OH and $[\text{CuCr}(\text{fsa})_2\text{en}(\text{H}_2\text{O})_2]\text{Cl}$, $3\text{H}_2\text{O}$ heterobinuclear complexes, where $(\text{fsa})_2\text{en}^{4-}$ denotes the bichelating ligand derived from the Schiff base *N,N'*(1-hydroxy, 2-carboxy benzilidene) ethylene diamine. The magnitude of the stabilization of the ground spin triplet with regard to the excited spin singlet in the former complex is explained in a topological way from the map of the overlap density. The accidental orthogonality may be predicted in planar di- μ -hydroxo copper(II) dimers with bridging angles around 92° , and in planar di- μ -azido copper(II) dimers with the azide ions bound end-on and bridging angles around 103° . A complex of this latter type was obtained, where the copper(II) ions are contained inside a cryptate cavity. The coupling is actually ferromagnetic.

Concerning the design of bridging or binucleating ligands particularly able to propagate the electronic effects between metal ions far away from each other, two examples are presented: derivatives of the dithioxamide in which two copper(II) ions separated by more than 5.6 Å may strongly interact through a $\text{C}_2\text{S}_2\text{N}_2$ bridging network and a copper(II) binuclear cryptate, in which the interaction occurs through two

azido groups bridged end-to-end. In both cases the mechanism of the interaction is specified.

Introduction

The aim of this work was to propose a strategy for designing polymetallic complexes exhibiting expected magnetic properties. Since the available place is limited, we shall focus on two aspects, namely the synthesis of complexes in which the metal ions are ferromagnetically coupled, and the preparation of complexes in which the metal ions are very strongly coupled in an antiferromagnetic manner, in spite of a large distance between them. In some way, we shall discuss the two extreme situations where the exchange parameter J is either positive or largely negative



The more classical situation of the antiferromagnetic interaction of medium magnitude between metal ions relatively close to each other has already been well documented [1].

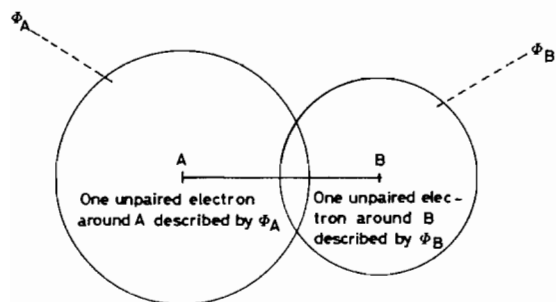
The first part of this paper will be devoted to the theoretical background; the second part will cover the ferromagnetic interaction, and the third part the antiferromagnetic interaction.

Theoretical Background

In this section, we restrict ourselves to the key concepts and relationships which will allow us to construct our strategy. This theoretical part is prima-

rily written for inorganic chemists looking for synthesizing themselves new coupled polymetallic complexes, and not for theoreticians.

Let us consider an A–B dimer, where A (or B) symbolizes a metallic ion surrounded by its terminal and bridging ligands. Let us also assume that there is just one unpaired electron around A and one unpaired electron around B. In the absence of interactions, the unpaired electron around A is described by a ϕ_A orbital, centered on the metal ion but partially delocalized towards the terminal and bridging ligands surrounding it. In the same way, the unpaired electron around B is described by ϕ_B . ϕ_A and ϕ_B are called *magnetic orbitals* [2].



The interaction between A and B leads to two molecular states, namely a spin singlet $S = 0$ and a spin triplet $S = 1$, separated by J . The interaction is antiferromagnetic if $S = 0$ is the ground state and J is negative. It is ferromagnetic if $S = 1$ is the ground state and J is positive.

If we make the following assumptions:

(i) the interaction is weak enough in order for the $S = 0$ and $S = 1$ states to be properly described by Heitler – London wavefunctions built from the magnetic orbitals;

(ii) the metal–metal charge transfer configuration of the type A^+B^- or A^-B^+ is much too high in energy to couple significantly with the ground configuration A – B,

then the singlet–triplet energy gap may be expressed in a relatively simple way as the sum of two components: an antiferromagnetic negative component J_{AF} , and a positive ferromagnetic component J_F :

$$J = J_{AF} + J_F \quad (1)$$

with [3]:

$$J_{AF} = -2S(\Delta^2 - \delta^2)^{1/2} \quad (2)$$

$$J_F = 2j \quad (3)$$

S is the overlap integral between the magnetic orbitals, j the two-electron exchange integral. If we

define the *overlap density* between the magnetic orbitals as [4]:

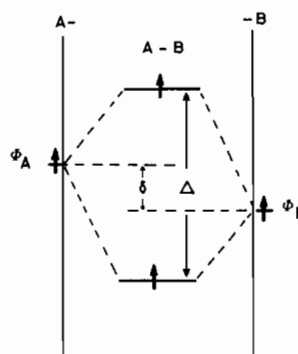
$$\rho(i) = \phi_A(i)\phi_B(i) \quad (4)$$

then S and j are given by:

$$S = \int_{\text{space}} \rho(i) d\tau_i \quad (5)$$

$$j = \int_{\text{space}} \frac{\rho(i)\rho(j)}{r_{ij}} d\tau_i d\tau_j \quad (6)$$

Δ is the energy gap between the two molecular orbitals in the A–B dimer constructed from the magnetic orbitals, for the $S = 1$ state. Finally δ is the energy gap between ϕ_A and ϕ_B as shown below:



If the A–B dimer is symmetrical, the A and B fragments are identical and δ is zero. J_{AF} is reduced to:

$$J_{AF} = -2\Delta S \quad (7)$$

The expressions (2) and (3) are obtained by expanding the eigenvalues of the true electrostatic Hamiltonian for the two active electrons in A–B, according to the increasing powers of S and by restricting the expansion to the terms in S .

So in our model the singlet–triplet energy gap J characterizing the nature and the magnitude of the exchange results from the competition between two *driving forces*, the one favouring the singlet state as ground state, characterized by J_{AF} , and the other one favouring the triplet state as ground state, characterized by J_F . J_{AF} , in absolute value, depends on the overlap S between the magnetic orbitals and on the energy gap $(\Delta^2 - \delta^2)^{1/2}$. In first order approximation, $(\Delta^2 - \delta^2)^{1/2}$ and S are proportional, so that J_{AF} roughly varies as $-S^2$ or $-(\Delta^2 - \delta^2)$. In the case $A = B$, Hoffmann *et al.* derived the same dependence of J_{AF} versus Δ^2 from a different approach [5]. J_F is related to the two-electron

exchange integral j , a well known result in atomic spectroscopy.

The simplest situation (but of course the least interesting from an experimental viewpoint) is obtained when the relative orientation of the magnetic orbitals is unfavourable to interaction. The overlap density ρ is then negligible in any point of the space and in (2) and (3), S , j and the two components J_{AF} and J_F are zero. The magnetic properties, therefore, are only the sum of what is expected for the A and B fragments.

Another relatively simple situation from a theoretical viewpoint but of the utmost importance experimentally is that where, in spite of $\rho \neq 0$, S is zero. In this case the antiferromagnetic component vanishes and the experimentally observed J energy gap reduces itself to its ferromagnetic component J_F . This situation corresponds to the orthogonality of the magnetic orbitals. We shall see later on that this orthogonality may be strict (owing to the symmetry of the problem), or accidental. We content ourselves to notice here that in the first order approximation where Δ and S are proportional (in the case $A = B$), the orthogonality of the magnetic orbitals leads to $\Delta = 0$.

The most frequently encountered situation is that where the J_{AF} component predominates. When the antiferromagnetic interaction is extremely strong, the pure Heitler-London wavefunctions may be no longer appropriate to describe the $S = 0$ and $S = 1$ low lying states. The borderline case is achieved when the molecular orbital description properly describes the $S = 0$ and $S = 1$ states. The stabilization of the singlet state with regard to the triplet state is then Δ instead of $2\Delta S$. Such a very strong antiferromagnetic interaction requires a large Δ gap. In part III we shall explain how such a gap may be obtained, even in dimers where the metal ions are far away from each other.

2. Ferromagnetic Interaction

2.1. Strict Orthogonality of the Magnetic Orbitals

To introduce this section, we consider first the A-B binuclear complex shown hereunder, obtained from the binucleating ligand noted $(fsa)_2en^{4-}$. Owing to the assymetry of the ligand, the A and B metal

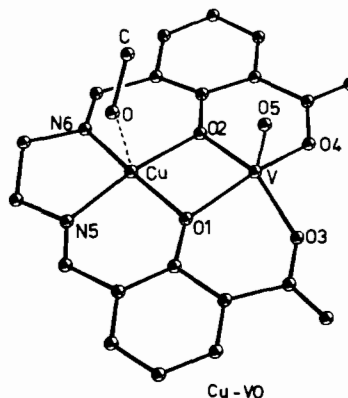
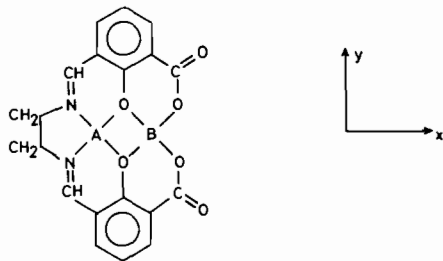


Fig. 1. Perspective view of $CuVO(fsa)_2en, CH_3OH$.

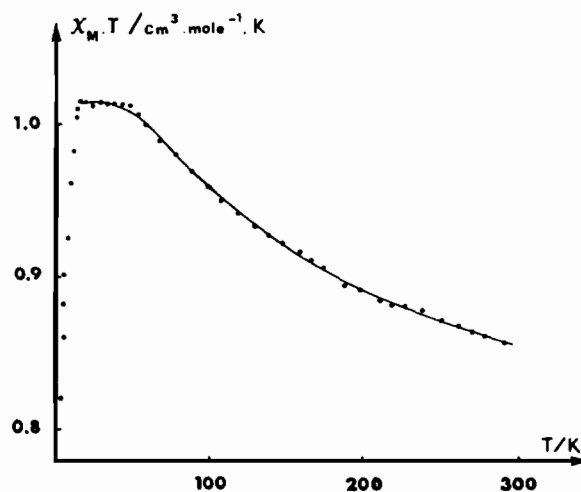


Fig. 2. Experimental (·) and theoretical (—) temperature dependence of $\chi_M T$ for $CuVO(fsa)_2en, CH_3OH$.

ions may be identical or different [6]. Figure 1 represents the crystal structure of the complex with $A = Cu(II)$ and $B = VO(II)$ [7]. The main feature of this structure lies in the fact that, at the accuracy of the experimental data, the metal ions, the oxygen atom of the methanol molecule weakly bound to $Cu(II)$, and the oxygen atom of the vanadyl group are all located in a plane which is a mirror for the two square pyramids CuN_2O_3 and VO_5 . It turns out that the symmetries of the metallic sites and the whole molecular symmetry are very close to C_s . The magnetic orbital ϕ_{Cu} centered on a $Cu(II)$ ion in a $4 + 1$ environment is constructed from the d_{xy} metallic orbital, and is partially delocalized towards the oxygen and nitrogen atoms surroundings the copper owing to the σ -type antibonding overlap ($d_{xy}|p_\sigma$). This magnetic orbital is therefore antisymmetric with regard to the $CuOVO$ mirror-plane. It transforms as the a'' irreducible representation of the C_s group. The magnetic orbital ϕ_{VO} is constructed from the

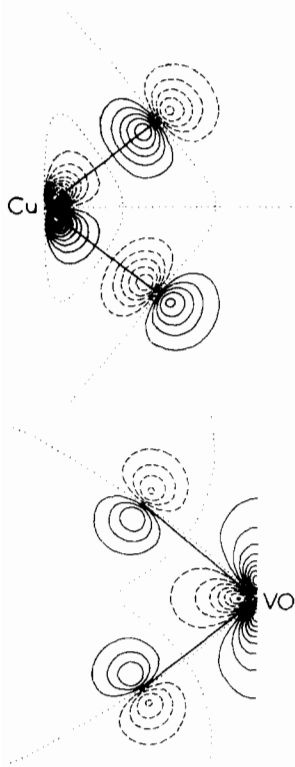


Fig. 3. Magnetic orbitals ϕ_{Cu} and ϕ_{VO} . The full lines represent the positive isovalue curves and the dashed lines the negative ones. The dotted lines represent the nodal zones.

$d_{x^2-y^2}$ metallic orbital and is partially delocalized towards the oxygen atoms of the pseudo molecular plane owing to the π -type antibonding overlaps $\langle d_{x^2-y^2} | p_{\pi} \rangle$. That magnetic orbital is symmetric with regard to the mirror-plane and transforms as a' . Thus the overlap integral $\langle \phi_{\text{Cu}} | \phi_{\text{VO}} \rangle$ is zero. There is no interaction favouring the pairing of the electrons. The singlet-triplet energy gap J is therefore given by:

$$J = 2j \quad (7)$$

which is a positive quantity.

The magnetic properties of this Cu(II)-VO(II) complex confirms that the coupling is actually ferromagnetic. These properties are represented in Fig.2 under the form of the variation of $\chi_{\text{M}}T$ versus T over the range $3.8 < T/\text{K} < 300$, χ_{M} being the molar magnetic susceptibility. Upon cooling from 300 K to around 50 K, $\chi_{\text{M}}T$ increases, then reaches a maximum and remains essentially constant down to 18 K, finally decreasing again below 18 K. Both Cu(II) and VO(II) ions have one unpaired electron and the exchange interaction leads to $S = 0$ and $S = 1$ states separated by J . The increase of $\chi_{\text{M}}T$ upon cooling

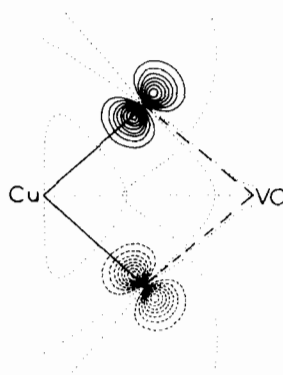


Fig. 4. Overlap density map in the CuO_2 plane of $\text{CuVO}(\text{fsa})_2\text{en}$, CH_3OH . The full lines represent the positive overlap density curves and the dashed lines the negative ones. The dotted lines represent the nodal zones. Differences in overlap density between two successive curves are similar.

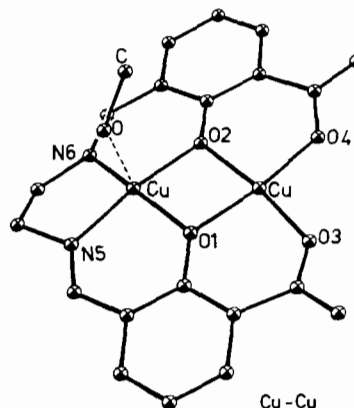


Fig. 5. Perspective view of $\text{Cu}_2(\text{fsa})_2\text{en}$, CH_3OH .

shows that the $S = 1$ level is the lowest in energy. Below 50 K, the $S = 0$ level is totally depopulated so that $\chi_{\text{M}}T$ is constant. The variation of $\chi_{\text{M}}T$ below 18 K is most likely due to an intermolecular anti-ferromagnetic coupling between the $S = 1$ molecular spins. The quantitative interpretation of the magnetic data leads to $J = 118 \text{ cm}^{-1}$ [7], which is actually a very large stabilization of the ground spin triplet.

Considering carefully not only the symmetries of the magnetic orbitals but also their relative orientations, we can understand why the coupling is so strongly ferromagnetic. Comparing ϕ_{Cu} and ϕ_{VO} represented in Fig. 3, one notices, in addition to their orthogonality, that the same 2p orbitals of the bridging oxygen atoms occur in ϕ_{Cu} , giving a σ overlap with d_{xy} centered on copper, and in ϕ_{VO} giving a π overlap with $d_{x^2-y^2}$ centered on vanadium. It turns out that the overlap density ρ presents two strongly positive lobes around one of the bridges, along the

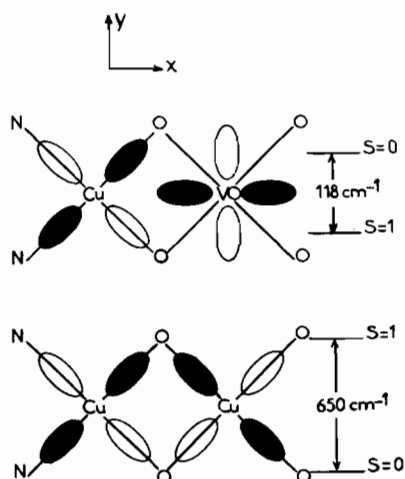


Fig. 6. Relative symmetries of the magnetic orbitals in $\text{CuVO}(\text{fsa})_2\text{en}, \text{CH}_3\text{OH}$ and $\text{Cu}_2(\text{fsa})_2\text{en}, \text{CH}_3\text{OH}$.

CuO axis and two strongly negative lobes around the other bridge. Figure 4 gives the overlap density map, plotted in the CuOO plane. Since the depth of the negative lobes (or holes) exactly compensates the altitude of the positive lobes (or summits), one has $S = 0$. On the other hand, the two-electron exchange integral j , the magnitude of which is essentially related to the extrema of ρ , summits or holes, may be important [4, 7].

A good way to see the heuristic character of this strategy of strict orthogonality to design ferromagnetically coupled systems is to compare $\text{CuVO}(\text{fsa})_2\text{en}, \text{CH}_3\text{OH}$ and $\text{Cu}_2(\text{fsa})_2\text{en}, \text{CH}_3\text{OH}$, the structure of which is shown in Fig. 5 [8]. In this latter complex the two magnetic orbitals have the same a'' symmetry. The overlap S is different from zero and the intramolecular interaction is strongly antiferromagnetic, the $S = 0$ level being 650 cm^{-1} lower in energy than the $S = 1$ level, as schematized in Fig. 6.

With a second example, we suggest that this strategy of strict orthogonality is of general applicability. Let us assume that with the same ligand $(\text{fsa})_2\text{en}^{4-}$, we have $A = \text{Cu(II)}$ in a $-\text{N}_2\text{O}_2$ planar environment and $B = \text{Cr(III)}$ in a pseudo octahedral environment, the coordination six being achieved by two molecules of solvent L as shown below:

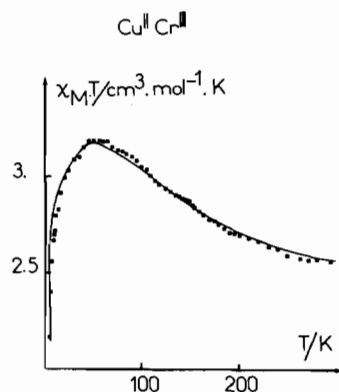
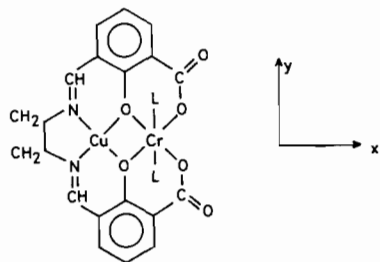


Fig. 7. Experimental () and theoretical (—) temperature dependences of $\chi_{\text{M}}T$ for $[\text{CuCr}(\text{fsa})_2\text{en}, (\text{H}_2\text{O})_2]\text{Cl}, 3\text{H}_2\text{O}$.

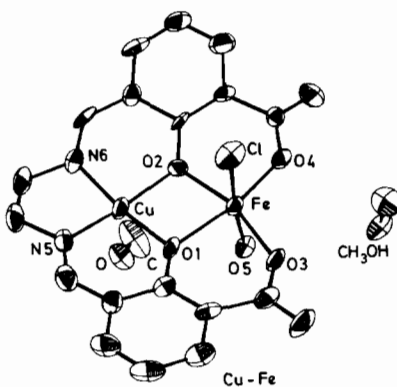
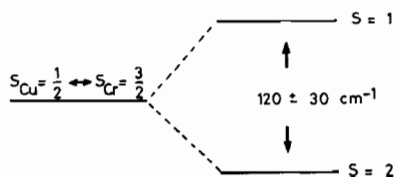


Fig. 8. Perspective view of $[\text{CuFe}(\text{fsa})_2\text{enCl}(\text{H}_2\text{O})], 2\text{CH}_3\text{OH}$.

The symmetries of the metal sites are very close to C_{2v} . It turns out that the unpaired electron around Cu(II) occupies an xy -type magnetic orbital transforming as b_1 , and that the three unpaired electrons around Cr(III) arising from the $(t_{2g})^3$ configuration occupy $x^2 - y^2$, xz and yz type magnetic orbitals transforming as a_1 , b_2 and a_2 respectively. The strict orthogonality is therefore again realized, so that a $\text{Cu(II)}-\text{Cr(III)}$ complex of this kind (if it does exist) should be ferromagnetically coupled, with the state of highest spin multiplicity $S = 2$ stabilized with regard to the state $S = 1$. We succeeded in synthesizing such a complex of formula $[\text{CuCr}(\text{fsa})_2\text{en}(\text{H}_2\text{O})_2]\text{Cl}, 3\text{H}_2\text{O}$ [9]. The variation of $\chi_{\text{M}}T$ versus T shown in Fig. 7 confirms that the coupling is ferromagnetic with the $S = 1$ state located at $120 \pm 30 \text{ cm}^{-1}$ above the $S = 2$ state, as shown below:



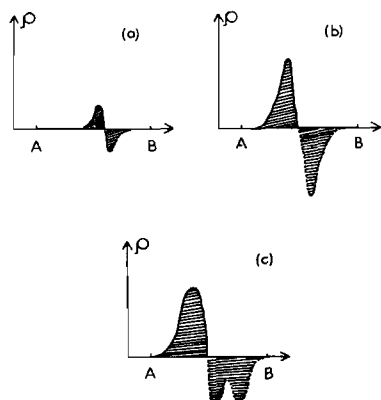


Fig. 9. Schematic variation of the overlap density in three cases of orthogonality of the magnetic orbitals: a: strict orthogonality and weak ferromagnetic interaction; b: strict orthogonality and strong ferromagnetic interaction; c: accidental orthogonality.

If we replace Cr(III) by Fe(III) in the B site, we obtain the complex Cu(II)–Fe(III), of which the structure is shown in Fig. 8. In a pseudo octahedral weak ligand field, the five magnetic orbitals around Fe(III) have the symmetries of the five d metal orbitals, i.e. $a_1(d_{z^2}$ and $d_{x^2-y^2})$, $a_2(d_{yz})$, $b_1(d_{xy})$ and $b_2(d_{xz})$. One of them, therefore, gives a non-zero overlap with the b_1 magnetic orbital around Cu(II). The strict orthogonality of the magnetic orbitals is destroyed and actually the coupling is antiferromagnetic with a $S = 2$ ground state and a $S = 3$ excited state located at some 290 cm^{-1} above [10].

2.2 Accidental Orthogonality of the Magnetic Orbitals

We attempted to specify in Fig. 9 what we call strict orthogonality and accidental orthogonality. The overlap density ρ is schematically plotted between the A and B metal centers. The cases *a* and *b* correspond to the *strict orthogonality* related to the symmetry properties of the complex and of the magnetic orbitals. In *a*, the overlap density presents itself in the form of an hill of weak altitude close to a shallow pond. In *b*, it presents itself in the form of a very high mountain close to a very deep sea. One clearly sees that *a* is associated to a weak ferromagnetic interaction and *b* to a strong ferromagnetic interaction. The case *c* corresponds to an *accidental orthogonality*, not directly related to the symmetry properties of the problem. For very peculiar values of the structural parameters, which cannot be known exactly *a priori*, the depth of the two ponds compensates the altitude of the summit so that $\int_{\text{space}} \rho(i) d\tau_i$ is equal to zero. Any structural deformation will destroy this accidental orthogonality, even if it does not change the molecular symmetry group [4].

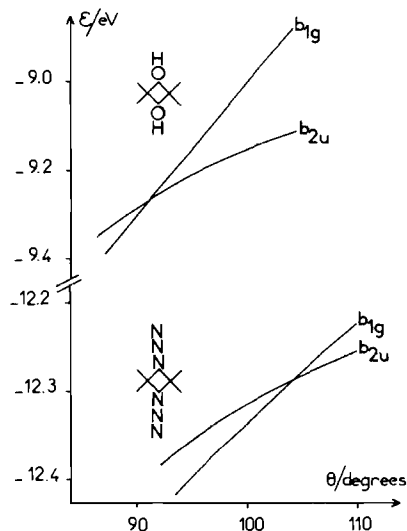
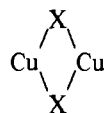


Fig. 10. Variations of the energies of the b_{1g} and b_{2u} molecular orbitals versus the bridging angle θ in planar di- μ -hydroxo copper(II) dimers and in planar di- μ -azido copper(II) dimers.

As it has been shown experimentally and discussed theoretically, the



planar network allows this situation of accidental orthogonality to occur [4, 5, 11]. This behaviour may be explained as follows: from the two magnetic orbitals of b_1 local symmetry one can construct two molecular orbitals transforming as b_{1g} and b_{2u} respectively. For a θ_0 value of the $\text{CuXCu} = \theta$ bridging angle, these m.o.'s are accidentally degenerate and the energy gap Δ involved in the relation (7) is zero. For $\theta < \theta_0$, b_{2u} is higher in energy than b_{1g} . For $\theta > \theta_0$ the opposite situation holds. When the X bridges are very electronegative, the s valence orbitals of the bridges are too low in energy to interact with the d_{xy} metal orbitals and θ_0 is very close to 90° . When X is made less electronegative, the $d_{xy} - s$ separation decreases. This interaction destabilizes b_{2u} with regard to b_{1g} , hence shifts θ_0 to larger θ . Assuming that Δ varies as S, we can assert that θ_0 corresponds to the value of the bridging angle for which the magnetic orbitals are accidentally orthogonal.

For $\text{X} = \text{OH}^-$, the orthogonality occurs for a θ_0 value around 90° , so that for any $\theta > 97.5^\circ$ the J_{AF} component is predominant and the observed coupling is antiferromagnetic. On the contrary, for any $\theta < 97.5^\circ$, J_{F} is the dominant component and the observed coupling is ferromagnetic [11]. If we replace the OH^- bridges by less electronegative

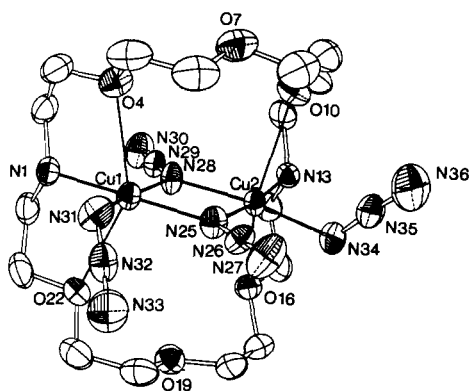
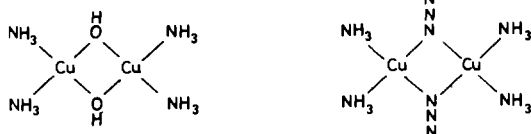
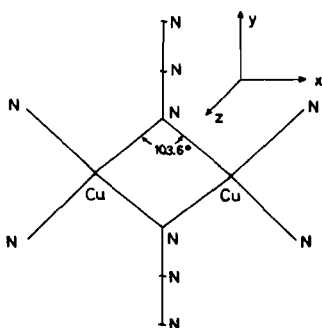


Fig. 11. Perspective view of the complex $\text{Cu}_2(\text{N}_3)_4(\text{C}_{16}\text{H}_{34}\text{N}_2\text{O}_6)$.

bridges like N_3^- with a terminal nitrogen atom linking two $\text{Cu}(\text{II})$ ions, θ_0 is expected at larger θ . Figure 10 shows the variations of the energies of the b_{1g} and b_{2u} m.o.'s against θ for the two model complexes:



as obtained by Extended Hückel calculations. The crossing point is calculated to $\theta_0 = 92^\circ$ for $\text{X} = \text{OH}^-$ and $\theta_0 = 103^\circ$ for $\text{X} = \text{N}_3^-$. It turns out that for di- μ -azido copper(II) dimers with $\text{Cu}-\text{N}-\text{Cu}$ bridging angles close to 103° , an intramolecular ferromagnetic coupling may be expected. Such a dimer is shown in Fig. 11 where azido groups and $\text{Cu}(\text{II})$ ions are contained inside a cryptate cavity. The skeleton relevant to discuss the magnetic properties is specified below:



The CuNcCu bridging angle is 103.6° and the coupling is actually ferromagnetic, as proved by the magnetic behaviour shown in Fig. 12. The ground spin triplet is stabilized by $70 \pm 20 \text{ cm}^{-1}$ with regard to the excited spin singlet [12].

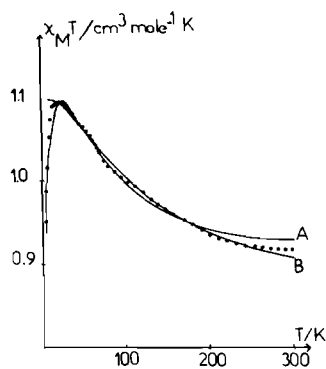


Fig. 12. Experimental (\cdot) and theoretical (—) temperature dependences of $\chi_M T$ for $\text{Cu}_2(\text{N}_3)_4(\text{C}_{16}\text{H}_{34}\text{N}_2\text{O}_6)$. Two methods, noted A and B respectively, were used to fit the experimental data (see Ref. [12]).

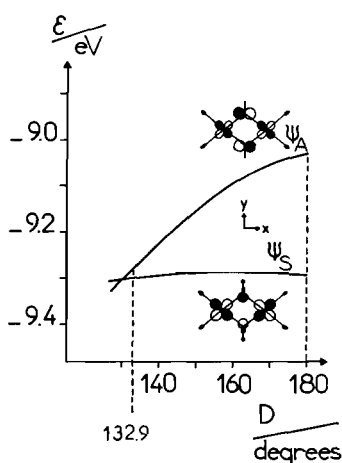
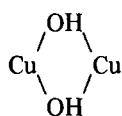


Fig. 13. Variation versus the dihedral angle D of the energies of the ψ_A and ψ_S molecular orbitals for roof shaped hydroxo-bridged $\text{Cu}(\text{II})$ dimers with $2 \text{ CuOO} = 105^\circ$.

We would like to propose another way to obtain the accidental orthogonality of the magnetic orbitals. Let us start from a planar



network, with a large CuOCu angle, say 105° . For this angle, the b_{1g} m.o. is largely destabilized with regard to b_{2u} and Δ is large. Now, let us bend the molecule along the $\text{O}-\text{O}$ direction, in the same way as one bends a book, the $\text{Cu}-\text{O}$ and $\text{O}-\text{O}$ distances remaining unchanged. The molecular symmetry center disappears, but the mirror-plane containing the $\text{O}-\text{O}$ direction is kept, so that it is appropriate to label the molecular orbitals ϕ_A and ϕ_S according

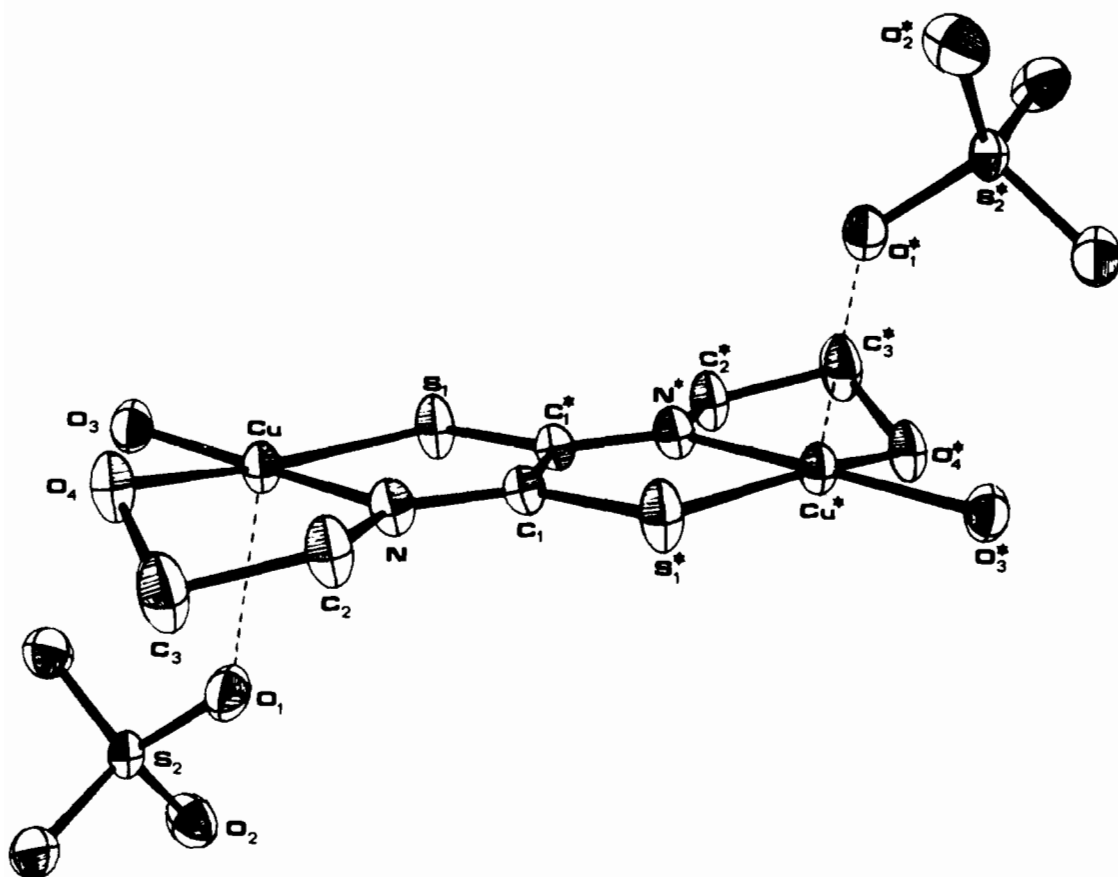


Fig. 14. Perspective view of $\{\text{Cu}_2[\text{S}_2\text{C}_2(\text{NCH}_2\text{CH}_2\text{OH})_2](\text{H}_2\text{O})_2\}\text{SO}_4$.

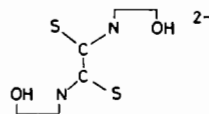
to whether they are antisymmetric or symmetric with regard to this mirror-plane (see Fig. 13). The copper-oxygen antibonding overlap decreases in absolute value in ϕ_A and remains constant in ϕ_S . It turns out that the energy of ϕ_A decreases and that of ϕ_S is almost unchanged. Therefore, a crossover is expected for a dihedral angle D between two CuO_2 planes smaller than 180° . In other words, starting from a planar hydroxo-bridged copper(II) dimer with a large overlap between the magnetic orbitals, one can expect an accidental zero overlap by bending the molecule along the O-O direction, and achieve a ferromagnetic coupling. Of course, such a deformation is easier to describe than to do. However, we checked that, everything else being unchanged, the smaller the dihedral angle is in a roof-shaped hydroxo-bridged copper(II) dimer, the weaker is the magnitude of the antiferromagnetic coupling [13]. In our example where we started from a planar network with $\text{CuOCu} = 105^\circ$, the accidental orthogonality of the magnetic orbitals is expected from an Extended Hückel calculation for a dihedral angle D of 130° (see Fig. 13). In the complex tetrakis (methylamine) di- μ -hydroxo dicopper(II) sulfate

monohydrate $[\text{Cu}(\text{CH}_3\text{NH}_2)_2\text{OH}]_2\text{SO}_4 \cdot \text{H}_2\text{O}$, D is 132.9° and the coupling is found to be very weakly antiferromagnetic with $J = -7.9 \pm 0.5 \text{ cm}^{-1}$ [14, 15]. To achieve a ferromagnetic coupling using this method, we need to bend the molecule by a few additional degrees.

3. Antiferromagnetic Interaction between Metal Ions far away from Each Other

The best way to show how it is possible to obtain a very large antiferromagnetic interaction between two metal ions far away from each other is to discuss some typical examples.

The first example deals with the binuclear complex $\{\text{Cu}_2[\text{S}_2\text{C}_2(\text{NCH}_2\text{CH}_2\text{OH})_2](\text{H}_2\text{O})_2\}\text{SO}_4$, the structure of which is given in Fig. 14. The molecular entity is dimeric with two $\text{Cu}(\text{II})$ ions separated by 5.61 Å, the bridging group being:



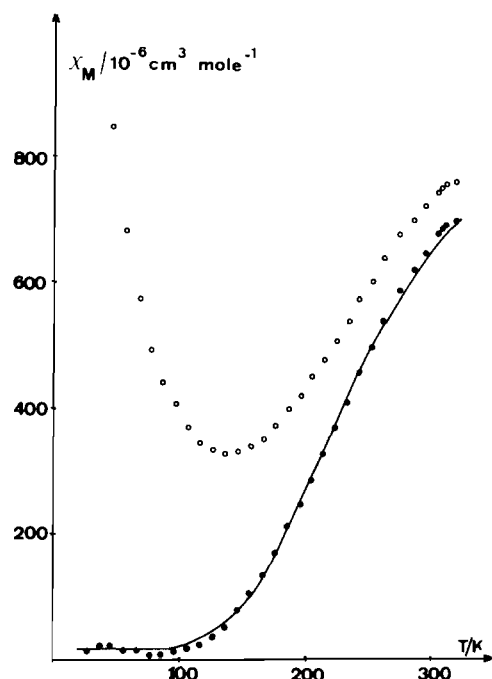


Fig. 15. Experimental and theoretical temperature dependence of the molar magnetic susceptibility χ_M for $\{\text{Cu}_2[\text{S}_2\text{C}_2(\text{NCH}_2\text{CH}_2\text{OH})_2](\text{H}_2\text{O})_2\}\text{SO}_4$ (○) experimental points, (●) points corrected of the noncoupled Cu(II) impurity, (—) theoretical curves.

In spite of the large metal–metal separation, the intramolecular antiferromagnetic interaction is very strong, as revealed by the susceptibility *versus* temperature plot shown in Fig. 15. The ground spin singlet is stabilized by 594 cm^{-1} with regard to the excited spin triplet [16].

The $-\text{O}_2\text{NS}$ surrounding of each Cu(II) ion is essentially planar, so that the magnetic orbitals are constructed from the d metal orbitals pointing towards the nearest neighbour atoms. The last occupied in-plane (σ) molecular orbitals for the bridging ligand are very close in energy to the d metal orbital, so that the metal–ligand interaction is important and the magnetic orbitals are strongly delocalized towards the nitrogen and sulfur atoms. The delocalization towards sulfur is particularly favoured owing to both the weak electronegativity of the element and the large diffuseness of its 3p orbitals. By combining the magnetic orbitals according to the symmetry properties of the problem, one obtains the a_g and a_u molecular orbitals schematized in Fig. 16. In the dimeric entity, the distance between the nitrogen and the sulfur atoms located on both sides of a carbon atom is only 2.68 \AA , so that the S–N overlap may be important. This overlap is itself favoured by the diffuseness of the 3p sulfur orbitals. Consequently the a_u m.o. in which the S–N overlaps are positive is significantly lower in

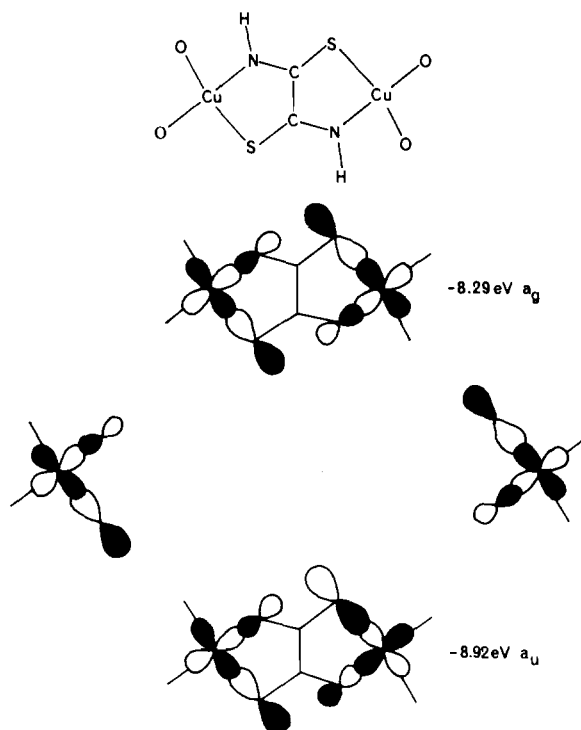


Fig. 16. Schematic representation of the magnetic orbitals and of the molecular orbitals built from these magnetic orbitals for the Cu(II) dimers with the $\text{C}_2\text{S}_2\text{N}_2$ bridging network.

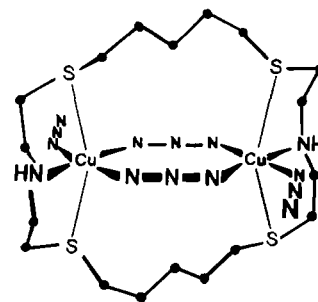
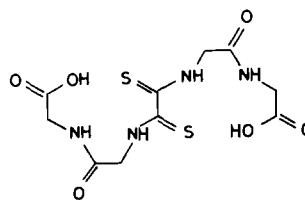


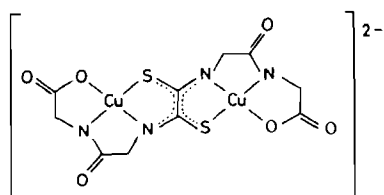
Fig. 17. Molecular structure of $\text{Cu}_2(\text{N}_3)_4(\text{C}_{18}\text{H}_{38}\text{N}_2\text{S}_4)$.

energy than the a_g m.o. in which the S–N overlaps are negative, and the Δ energy gap may be as large as 0.63 eV .

Other ligands with the same $\text{S}_2\text{C}_2\text{N}_2$ bridging group were synthesized. All lead to strongly antiferromagnetically coupled Cu(II) dimers [17]. One of these ligands, prepared by the action of the glycylglycine on the dithiooxamide, is:



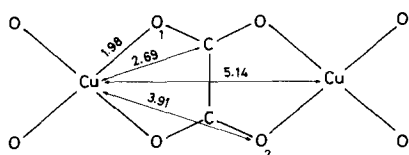
With Cu(II), it gives the complex hereunder for which $J = -630 \text{ cm}^{-1}$ [18].



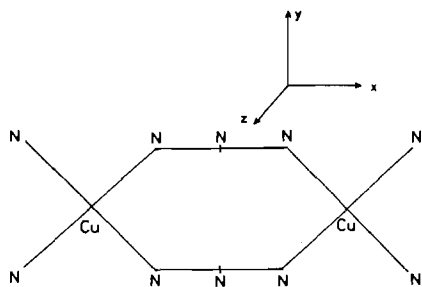
To summarize, the magnitude of the antiferromagnetic interaction between the two Cu(II) ions through the $\text{C}_2\text{S}_2\text{N}_2$ bridge is due to:

(i) the proper relative orientations of the singly occupied d metal orbitals and of the last occupied in-plane σ ligand orbitals;

(ii) the weak electronegativity of the sulfur atom and the large diffuseness of its valence orbitals. It is easy to check that if the second condition disappears, then the coupling becomes weaker. So the interaction between two Cu(II) ions separated by 5.14 Å through the oxalato bridge (see hereunder) is characterized by $J = -291 \text{ cm}^{-1}$ [19, 20].



The second example will deal with another di- μ -azido copper(II) dimer, but with the azido groups bridging in an end-to-end fashion. Such a complex has been described by Weiss *et al.* [21]. The metal ions and the two azido groups are again contained inside a cryptate cavity. Its structure is shown in Fig. 17. The skeleton relevant for discussion of the magnetic properties is represented hereunder. All the atoms of this skeleton are coplanar.



We idealized somewhat the geometry by assuming a D_{2h} molecular symmetry. In spite of a copper-copper separation of 5.14 Å, the complex is diamagnetic in the whole temperature range 4.2–390 K. This means that the singlet–triplet energy gap J is too large in absolute value to be measured by the magnetic susceptibility techniques. The two Cu(II) ions are therefore very strongly coupled in an antiferromagnetic manner.

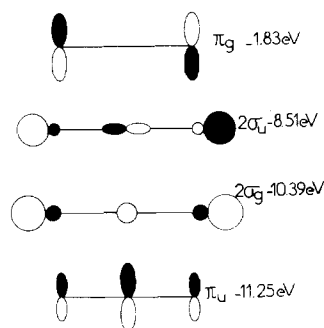


Fig. 18. The six highest occupied molecular orbitals in the azido ion.

The d metal orbital of highest energy for each Cu(II) ion is d_{xy} , occupied by the unpaired electron and pointing towards the terminal and bridging nitrogen atoms. The six highest occupied molecular orbitals for the azido ligand are represented in Fig. 18 [22]. The essentially non-bonding π_g level is much higher in energy than $2\alpha_u$, $2\sigma_g$ and π_u levels just below. It turns out that the energy difference between metal d_{xy} orbitals and ligand orbitals is much weaker for the couple $d_{xy} - \pi_g$ than for the couples $d_{xy} - 2\alpha_u$, $d_{xy} - 2\sigma_g$ or $d_{xy} - \pi_u$, so that the interaction $d_{xy} - \pi_g$ is preponderant. This interaction leads to molecular orbitals transforming as b_{1g} in the group D_{2h} . These m.o.'s are antisymmetric regarding the $\sigma(yz)$ mirror-plane. The interaction $d_{xy} - 2\sigma_u$ leads to m.o.'s of the same b_{1g} symmetry. Thus, owing to the $\pi_g - 2\sigma_u$ hybridisation in the D_{2h} group, we shall have three b_{1g} m.o.'s, one very low in energy, the second one weakly bonding (or weakly antibonding) and the last one, noted ϕ_A , very high in energy. In the same way, the $2\sigma_g$ and π_u levels of the azido bridges hybridise themselves in D_{2h} to interact with d_{xy} , giving rise to three m.o.'s transforming as b_{2u} and antisymmetric regarding the $\sigma(yz)$ mirror plane; one is slightly stabilized with regard to π_u , the second one is essentially non-bonding and the third one (noted ϕ_S) is slightly destabilized with regard to d_{xy} . This correlation between metallic levels and ligand levels is schematized in Fig. 19, where, for the sake of simplicity,

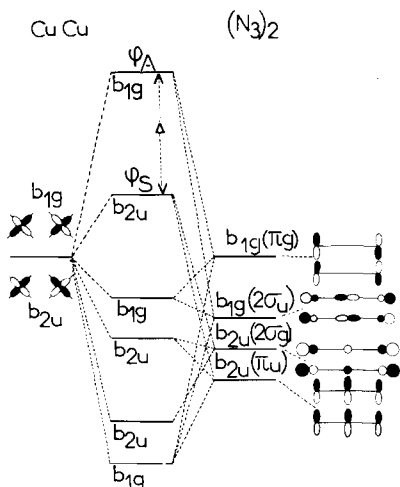


Fig. 19. Correlation between metal levels and ligand levels for $\text{Cu}_2(\text{N}_3)_4(\text{C}_{18}\text{H}_{38}\text{N}_2\text{S}_4)$.

we ignored the ligand levels not interacting with d_{xy} and the other metallic orbitals. The energy gap Δ governing the magnitude of the antiferromagnetic coupling is defined by $\Delta = \epsilon(\phi_A) - \epsilon(\phi_S)$. Owing to the $d_{xy} - \pi_g$ interaction between levels close in energy, Δ is very large. We represented ϕ_A and ϕ_S as obtained by Extended Hückel Calculation in Fig. 20. Δ was found equal to 1.10 eV [12]

Conclusion

It is difficult to conclude work which is still in progress. The main directions in which we would like to advance are: (i) a best control of the structural parameters leading to the accidental orthogonality of the magnetic orbitals; (ii) the utilization of this strategy of orthogonality to design one-dimensional ferromagnets; (iii) the synthesis of new sulfur-containing binucleating ligands particularly appropriate to propagate the electronic effects on long distances. At this stage of our work we believe to have shown that the main factors governing the nature and the magnitude of the exchange interaction in polynuclear systems are today relatively well understood. It is now possible to predict what kinds of transition ions, of terminal and bridging ligands we have to use, what kinds of local and whole symmetries we have to design when we want to obtain a new complex exhibiting expected magnetic properties.

Acknowledgement

I wish to express my deep gratitude to all my co-workers. To a large extent, the work described above

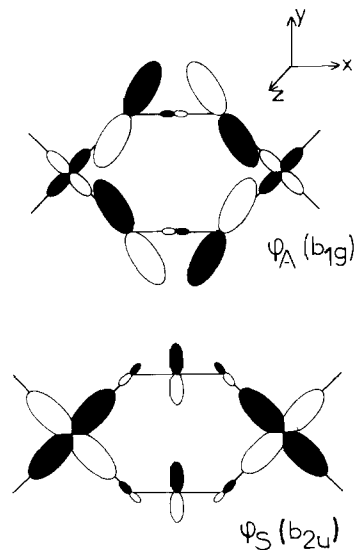


Fig. 20. Schematic representation of the ϕ_S and ϕ_A molecular orbitals for $\text{Cu}_2(\text{N}_3)_4(\text{C}_{18}\text{H}_{38}\text{N}_2\text{S}_4)$.

belongs to them. Their names appear in the references listed.

References

- 1 See for instance, A. P. Ginsberg, *Inorg. Chim. Acta Rev.*, **5**, 45 (1971); L. V. Interrante, 'Extended Interactions between Metal Ions in Transition Metal Complexes', Chaps. 8, 9, 10, 11, 14, 16, A.C.S. Symposium Series No. 5 (1974).
- 2 J. J. Girerd, M. F. Charlot and O. Kahn, *Mol. Phys.*, **34**, 1063 (1977); J. J. Girerd, Y. Journaux and O. Kahn, *Chem. Phys. Letters*, **82**, 534 (1981).
- 3 P. Tola, O. Kahn, C. Chauvel and H. Coudanne, *Nouv. J. Chim.*, **1**, 467 (1977).
- 4 O. Kahn and M. F. Charlot, *Nouv. J. Chim.*, **4**, 567 (1980).
- 5 P. J. Hay, J. C. Thibeault and R. Hoffmann, *J. Am. Chem. Soc.*, **97**, 4884 (1975).
- 6 U. Casellato, P. A. Vigato, D. E. Fenton and M. Vidali, *Chem. Soc. Rev.*, **8**, 199 (1979).
- 7 O. Kahn, J. Galy, Y. Journaux, J. Jaud and I. Morgenstern-Badarau, *J. Am. Chem. Soc.*, **104**, 2165 (1982).
- 8 J. Galy, J. Jaud, O. Kahn and P. Tola, *Inorg. Chim. Acta*, **36**, 229 (1979).
- 9 Y. Journaux and O. Kahn, *Angew. Chem. Int. Ed.*, in press.
- 10 J. Jaud, Y. Journaux, J. Galy and O. Kahn, *Nouv. J. Chim.*, **4**, 629 (1980).
- 11 V. M. Crawford, H. W. Richardson, J. R. Wasson, D. J. Hodgson and W. E. Hatfield, *Inorg. Chem.*, **15**, 2107 (1976).
- 12 J. Comarmond, P. Plumere, J. M. Lehn, Y. Agnus, R. Louis, R. Weiss, O. Kahn and I. Morgenstern-Badarau, *J. Am. Chem. Soc.*, in press.
- 13 M. F. Charlot, S. Jeannin, Y. Jeannin, O. Kahn, J. Lucrece Abaul and J. Martin-Frere, *Inorg. Chem.*, **18**, 1675 (1979).

- 14 Y. Litaka, K. Shimizu and T. Kwan, *Acta Crystallogr.* **20**, 803 (1966).
- 15 M. F. Charlot, O. Kahn, S. Jeannin and Y. Jeannin, *Inorg. Chem.*, **19**, 1410 (1980).
- 16 J. J. Girerd, S. Jeannin, Y. Jeannin and O. Kahn, *Inorg. Chem.*, **17**, 3034 (1978).
- 17 C. Chauvel, J. J. Girerd, Y. Jeannin and G. Lavigne, *Inorg. Chem.*, **18**, 3015 (1979).
- 18 J. J. Girerd and O. Kahn, *Angew. Chem. Int. Ed.*, **21**, 385 (1982).
- 19 A. Michalowicz, J. J. Girerd and J. Goulon, *Inorg. Chem.*, **18**, 3004 (1979).
- 20 J. J. Girerd, O. Kahn and M. Verdaguer, *Inorg. Chem.*, **19**, 274 (1980).
- 21 Y. Agnus, R. Louis and R. Weiss, *J. Am. Chem. Soc.*, **101**, 3381 (1979).
- 22 J. F. Wyatt, I. H. Hillier, V. R. Saunders, J. A. Connor and M. Barber, *J. Chem. Phys.*, **54**, 5311 (1971).